

Vehicle predictive trajectory patterns from isochronous data

Dumitru Damian

Engineering Consultant

Deva, 33012, RO

DUMITRUDAMIAN@YAHOO.COM

Editor: open

Abstract

Measuring and analyzing sensor data is the basic technique in vehicle dynamics development and with the advancement of embedded and data acquisition systems it is possible to analyze large data sets. In this paper a detailed method is presented for assessing and mapping isochronous trajectory patterns in Graz (Austria) by using data fusion from video, ArduinoUno and the compass sensor HDMM01. The predictive isochronous trajectory patterns are derived from the data values for a predefined time horizon. Both extreme driving behavior and hazardous road geometries can be identified. It is possible to provide instant road sensor data which can be used to compare the data from a trajectory path as well as for different time instances. Results of this study show that the trajectory patterns are successful in predicting the likely evolution of a current trajectory pattern and can provide assessment on future driving situations. The obtained data from this study can be useful as reference in future city planning for energy saving driving pathways as well as vehicle design and engineering improvements based on quantitative and relevant dynamic measurements.

Keywords: Dynamics, Transport, Online, Isochronous Trajectory, Compass, Arduino UNO, Data Analysis, Sensor, Vehicle, ADAS, Road Geometry, Estimation, HDMM01

1. Introduction

Predicting vehicle behavior is a major challenge and an active research domain for the automotive industry. The desire to develop intelligent vehicles that make good use of predictive vehicle behavior and contribute to the improvement of road safety can find a possible implementation by using the low cost compass sensor data.

Complex planning algorithms have begun to factor in uncertainty that arise from variations in travel time, erratic communication between autonomous vehicles, imperfect sensor data or other situations. To consider such scenarios, a method for path planning is developed that also generates contingency vehicle paths, should the initial path prove too risky. By using the isochronous trajectory patterns it is also possible to identify particular conditions that consider sensor readings or delays in the measured data, that must trigger a switch to a particular contingency vehicle path.

The isochronous trajectory is defined to be a sequence of position vectors in the 3-dimensional Euclidean space, the notation used is Γ and has the following representation:

$$\Gamma_t = (x_t, y_t, z_t)$$

where $t=20\text{ms}$.

The coordinate system used in vehicle dynamics modeling is according to SAE J670e as shown in Figure 2.

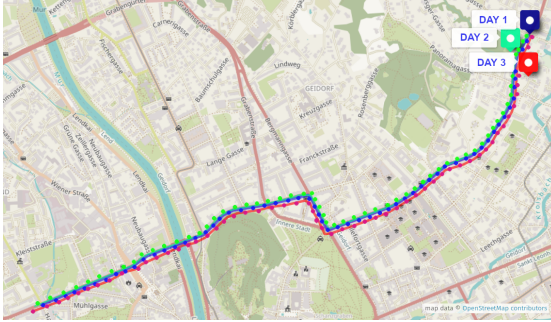


Figure 1: Vehicle path with isochronous data

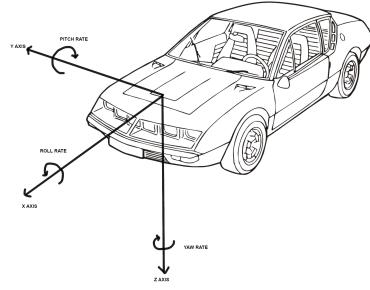


Figure 2: Vehicle axis system

From the vehicle axis system it is possible to construct the isochronous surface. The X, Y and Z direction can be represented by one or multiple nodes that describe the isochronous surface.

The vehicle is considered to be a rigid body, the position vector for a point P in the XYZ coordinates system, will have the following representation:

$$\vec{r} = \vec{r}_t$$

$$\vec{r} = x_t * \vec{i} + y_t * \vec{j} + z_t * \vec{k}$$

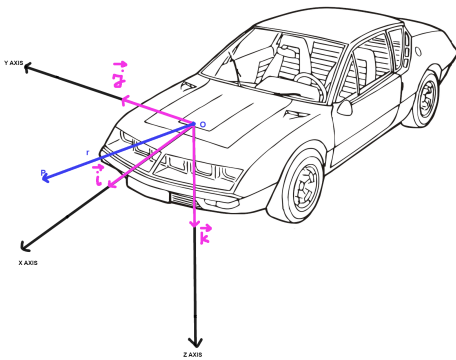


Figure 3: OP positional vector

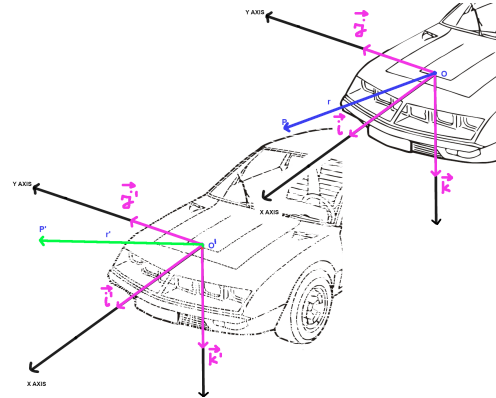


Figure 4: O'P' vector with new coordinates

The position vector for a point P' in the mobile X'Y'Z' coordinates system can be localized trough:

$$\vec{r}' = \vec{r}'_t$$

$$\vec{r}' = x'_t * \vec{i}' + y'_t * \vec{j}' + z'_t * \vec{k}'$$

Also, the origin O' for the mobile X'Y'Z' coordinates system in comparison with the origin O for the XYZ coordinates system can be represented trough the position vector:

$$\vec{r}_0 = \vec{r}_{0t}$$

$$\vec{r}_0 = x_{0_t} * \vec{i} + y_{0_t} * \vec{j} + z_{0_t} * \vec{k}$$

and thus:

$$\vec{r}_t = \vec{r}_{0_t} + \vec{r}'_t$$

The relation between \vec{r}'_t and \vec{r}_t can be represented through the following relation:

$$i' = \alpha_{11} * i + \alpha_{12} * j + \alpha_{13} * k$$

$$j' = \alpha_{21} * i + \alpha_{22} * j + \alpha_{23} * k$$

$$k' = \alpha_{31} * i + \alpha_{32} * j + \alpha_{33} * k$$

And from this dependency the isochronous matrix that characterizes the state change for one time step is determined:

$$A = \begin{pmatrix} \alpha_{11} & \alpha_{12} & \alpha_{13} \\ \alpha_{21} & \alpha_{22} & \alpha_{23} \\ \alpha_{31} & \alpha_{32} & \alpha_{33} \end{pmatrix}$$

From the above representation it is possible to derive the velocity isochronous matrix:

$$\begin{aligned} \vec{v} &= \frac{d\vec{r}}{dt} = \dot{\vec{r}} = \frac{d\vec{r}_0}{dt} + \frac{d\vec{r}'_t}{dt} = \dot{\vec{r}}_0 + \dot{\vec{r}}'_t \\ \dot{\vec{r}}_0 &= x_{0_t} \dot{\vec{i}} + y_{0_t} \dot{\vec{j}} + z_{0_t} \dot{\vec{k}} \\ \dot{\vec{r}}'_t &= \dot{x}' \dot{\vec{i}}' + \dot{y}' \dot{\vec{j}}' + \dot{z}' \dot{\vec{k}}' \end{aligned}$$

Each isochronous surface can have multiple nodes that characterize the state of respective surface. For one mini-node, the vehicle velocity isochronous matrix can be represented:

$$V = \begin{pmatrix} v_{11} & v_{12} & v_{13} \\ v_{21} & v_{22} & v_{23} \\ v_{31} & v_{32} & v_{33} \end{pmatrix} \quad (1)$$

The equation (1) can be applied to each mini-node that forms the isochronous surface. For when there are 9 mini-nodes, the vehicle velocity isochronous matrix will be:

$$V_{iso} = \begin{pmatrix} \begin{pmatrix} v_{111} & v_{112} & v_{113} \\ v_{121} & v_{122} & v_{123} \\ v_{131} & v_{132} & v_{133} \end{pmatrix} & \begin{pmatrix} v_{211} & v_{212} & v_{213} \\ v_{221} & v_{222} & v_{223} \\ v_{231} & v_{232} & v_{233} \end{pmatrix} & \begin{pmatrix} v_{311} & v_{312} & v_{313} \\ v_{321} & v_{322} & v_{323} \\ v_{331} & v_{332} & v_{333} \end{pmatrix} \\ \begin{pmatrix} v_{411} & v_{412} & v_{413} \\ v_{421} & v_{422} & v_{423} \\ v_{431} & v_{432} & v_{433} \end{pmatrix} & \begin{pmatrix} v_{511} & v_{512} & v_{513} \\ v_{521} & v_{522} & v_{523} \\ v_{531} & v_{532} & v_{533} \end{pmatrix} & \begin{pmatrix} v_{611} & v_{612} & v_{613} \\ v_{621} & v_{622} & v_{623} \\ v_{631} & v_{632} & v_{633} \end{pmatrix} \\ \begin{pmatrix} v_{711} & v_{712} & v_{713} \\ v_{721} & v_{722} & v_{723} \\ v_{731} & v_{732} & v_{733} \end{pmatrix} & \begin{pmatrix} v_{811} & v_{812} & v_{813} \\ v_{821} & v_{822} & v_{823} \\ v_{831} & v_{832} & v_{833} \end{pmatrix} & \begin{pmatrix} v_{911} & v_{912} & v_{913} \\ v_{921} & v_{922} & v_{923} \\ v_{931} & v_{932} & v_{933} \end{pmatrix} \end{pmatrix} \quad (2)$$

By considering multiple isochronous surfaces it is possible to have complex predictive trajectory paths.

2. Random segmentation surfaces for isochronous trajectories

It is also possible to define a specific isochronous surface type and flag such segmentation surfaces that lead to changes in the trajectory path. To that extent, for a random segmentation surface X , the following considerations are made:

- there are n values that characterize the segmentation surfaces S_1, S_2, \dots, S_n
- there are n surfaces dispersals $D^2(X_1), D^2(X_2), \dots, D^2(X_n)$ that characterize the segmentation surfaces distributions
- there are $n(n - 1)$ isochronous correlations defined as:

$$K_{ij} = V_{iso_{ij}}[(X_i - m_i)(X_j - m_j)]$$

where:

- X_i, X_j are the random segmentation surfaces
- m_i, m_j are the mean expected surface values
- $V_{iso_{ij}}$ is the vehicle velocity isochronous matrix specific to the respective random segmentation surfaces

For situations when it is required to determine the distribution of a random segmentation surface event from the trajectory path, a particular case of the correlation can be used:

$$D^2(X_i) = K_{ii} = V_{iso_{ij}}[(X_i - m_i)^2]$$

For the complete trajectory Γ it is possible to construct a correlations distribution matrix that describes the distribution of random segmentation surfaces S_1, S_2, \dots, S_n :

$$\Gamma_{ij} = \begin{pmatrix} K_{11} & K_{12} & \dots & K_{1n} \\ K_{21} & K_{22} & \dots & K_{2n} \\ \dots & \dots & \dots & \dots \\ K_{n1} & K_{n2} & \dots & K_{nn} \end{pmatrix}$$

Since the defined correlation allows the equality $K_{ij} = K_{ji}$, the distribution matrix will also contain this equality and can be represented in the following way:

$$\Gamma_{ij} = \begin{pmatrix} K_{11} & K_{12} & \dots & K_{1n} \\ & K_{22} & \dots & K_{2n} \\ & & \dots & \\ & & & K_{nn} \end{pmatrix}$$

As a consequence the isochronous trajectory is expanded to include the random segmentation surfaces and the correlation distribution matrix for them:

$$\Gamma_t = f \left((x_t, y_t, z_t), \begin{pmatrix} K_{11} & K_{12} & \dots & K_{1n} \\ & K_{22} & \dots & K_{2n} \\ & & \dots & \\ & & & K_{nn} \end{pmatrix} \right) \quad (3)$$

2.1 Domain of multiple random segmentation surfaces

It is well known that a geometric mesh represents the discretization of the geometric domain into smaller and simpler shapes. For the two dimension, the triangles and quadrilaterals meshes are used. For the tree dimensions, the tetrahedral and hexahedral meshes are used as defined by Bern and Plassmann (2000).

Since the trajectory path is a mesh of isochronous surfaces, based on previous recorded path data and the received node information, it is possible to detect path domains where movement obstacles might exist.

Such an obstacle domain can be broken down into groups of segmentation surfaces with various sizes. The spacing between such surfaces can be identical with the isochronous surfaces space. The boundary for the obstacle domain will be:

$$OBS = S_1 \cup S_2$$

where the S_1 and S_2 will have the following representation:

$$(S_1) \mapsto X = \zeta_1(Y, Z)$$

$$(S_2) \mapsto X = \zeta_2(Y, Z)$$

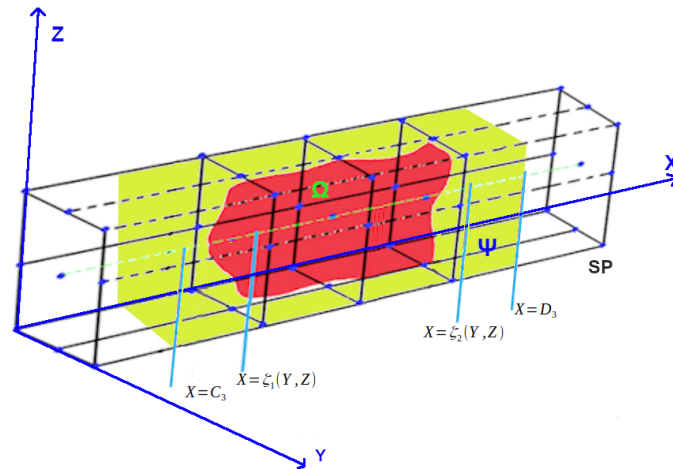


Figure 5: Trajectory segmentation surfaces create a domain in the future trajectory path where risks exists.

The obstacle domain is named as Ω and it is contained within the Ψ domain defined by the segmentation surface $X = C_3$ till $X = D_3$, where C_3 and D_3 are random surfaces that might or might not consider the time constraints that the isochronous surfaces follow.

From this representation it is possible to define a function that defines the movement through this section path SP. The resulting values can be found in the real numbers domain.

$$\hat{f} : SP \mapsto R$$

$$\hat{f}(x, y, z) = \begin{cases} f(x, y, z) & , \text{ if } (x, y, z) \in \Omega \\ 0 & , \text{ if } (x, y, z) \in \Psi / \Omega \end{cases}$$

From this it is possible to determine the function for the path section domain:

$$\begin{aligned} \iiint_{SP} \hat{f}(x, y, z) dx dy dz &= \iiint_{\Omega} \hat{f}(x, y, z) dx dy dz + \iiint_{\Psi} \hat{f}(x, y, z) dx dy dz \\ \iiint_{SP} \hat{f}(x, y, z) dx dy dz &= \iint_{SP_{YZ}} \left(\int_{C_3}^{D_3} \hat{f}(x, y, z) dx \right) dy dz \end{aligned}$$

Now it is possible to define the complete Ω domain and the Ψ domain following the X-axis:

$$\int_{C_3}^{D_3} \hat{f}(x, y, z) dx = \int_{C_3}^{\zeta_1(Y,Z)} \hat{f}(x, y, z) dx + \int_{\zeta_1(Y,Z)}^{\zeta_2(Y,Z)} \hat{f}(x, y, z) dx + \int_{\zeta_2(Y,Z)}^{D_3} \hat{f}(x, y, z) dx$$

Or only considering the Ω domain:

$$\int_{C_3}^{D_3} \hat{f}(x, y, z) dx = 0 + \int_{\zeta_1(Y,Z)}^{\zeta_2(Y,Z)} \hat{f}(x, y, z) dx + 0$$

Since the domain outside the Ω domain is minimized to the 0 value, it can be considered that:

$$\iiint_{SP} \hat{f}(x, y, z) dx dy dz = \iiint_{\Omega} f(x, y, z) dx dy dz$$

At the same time, if multiple path section domains are to be encountered, the trajectory using isochronous surfaces can be described as:

$$\iiint_{SP} f(x, y, z) dx dy dz = \sum_{q=1}^n \iiint_{\Omega_q} f(x, y, z) dx dy dz$$

From the defined isochronous surfaces it is possible to construct a trajectory mesh by using a mapping function. The coordinates of the nodes are known in the isochronous surface. The obtained mesh is then super imposed on the trajectory images.

As a consequence the isochronous trajectory is expanded to include the obstacle domain Ω :

$$\Gamma_t = f \left((x_t, y_t, z_t), \begin{pmatrix} K_{11} & K_{12} & \dots & K_{1n} \\ & K_{22} & \dots & K_{2n} \\ & & \dots & \\ & & & K_{nn} \end{pmatrix}, \hat{f}(x, y, z) \right) \quad (4)$$

2.2 Probability of segmentation surfaces

Since a possible change in the trajectory is initialized by the segmentation surface, the distribution of the trajectory change can be modeled using the Laplace–Gauss distribution.

The density of repartition is described in Moineagu (1976) as:

$$f(x; m; \sigma) = \frac{1}{\sigma\sqrt{2\pi}} e^{-\frac{1}{2} \frac{(x-m)^2}{\sigma^2}}$$

where:

- x real-valued random variable
- m maximum
- σ standard deviation

The probability that random segmentation surface S_n takes a value between (x_1, x_2) is given by:

$$P(x_1 < S_n < x_2) = \int_{x_1}^{x_2} f(x; m; \sigma) dx = \frac{1}{\sigma\sqrt{2\pi}} \int_{x_1}^{x_2} e^{-\frac{1}{2} \frac{(x-m)^2}{\sigma^2}} dx$$

If we make the variable change $y = \frac{x-m}{\sigma}$ then $x = \sigma y + m$, $dx = \sigma dy$.

- $x = x_1$ then $y = \frac{x_1-m}{\sigma}$
- $x = x_2$ then $y = \frac{x_2-m}{\sigma}$

$$P(x_1 < S_n < x_2) = \frac{\sigma}{\sigma\sqrt{2\pi}} \int_{\frac{x_1-m}{\sigma}}^{\frac{x_2-m}{\sigma}} e^{-\frac{y^2}{2}} dy = \frac{1}{\sqrt{2\pi}} \left(\int_{-\infty}^{\frac{x_2-m}{\sigma}} e^{-\frac{y^2}{2}} dy - \int_{-\infty}^{\frac{x_1-m}{\sigma}} e^{-\frac{y^2}{2}} dy \right)$$

If we consider the distribution function with the parameters 0 and 1, we can define the Laplace function Φ :

$$\Phi(x) = \int_{-\infty}^x f(y; 0; 1) dy = \frac{1}{\sqrt{2\pi}} \int_{-\infty}^x e^{-\frac{y^2}{2}} dy$$

and the probability that random segmentation surface S_n takes a value between (x_1, x_2) is given by:

$$P(x_1 < S_n < x_2) = \Phi\left(\frac{x_2 - m}{\sigma}\right) - \Phi\left(\frac{x_1 - m}{\sigma}\right)$$

As a consequence the isochronous trajectory is expanded to include the probability of random segmentation surfaces:

$$\Gamma_t = f\left((x_t, y_t, z_t), \begin{pmatrix} K_{11} & K_{12} & \dots & K_{1n} \\ & K_{22} & \dots & K_{2n} \\ & & \dots & \\ & & & K_{nn} \end{pmatrix}, \hat{f}(x, y, z), P(x_1 < S_n < x_2)\right) \quad (5)$$

3. Isochronous trajectory chords

Since it is possible to start from a node, follow an edge to the next node and then select another edge that is not adjacent to the first edge to continue to another edge, it is possible to define the concept of isochronous surface chords. They can be closed or open curves and can produce self-intersections.

Theorem 1 *If one of the chords is disturbed, the disturbance is instantaneous transmitted throughout the complete Γ_t .*

By observing the amplitude of the chords disturbance it will be possible to build predictive paths for the remaining trajectory while at the same time updating the already known path.

As previously defined, the isochronous trajectory Γ , is composed of isochronous surfaces that interact with each other through the chords. The Γ trajectory can be updated with new data from trajectories not yet travelled. The intent to change the already known Γ trajectory with another Γ trajectory, is captured by the "vibrations" of the isochronous surface chords defined as $\delta(t)$.

By analyzing the isochronous surface matrix of the velocity, acceleration and trajectory path updates it is possible to identify the isochronous surfaces that favour the appearance of chords vibrations.

$$\delta(t) = v_{m,n,p}(t) + \dot{v}_{m,n,p}(t) + \Omega_{m,n,p}(t)$$

where:

- m, n, p are the indexes of the mini-nodes for each isochronous surface
- $v_{m,n,p}(t)$ is the velocity
- $\dot{v}_{m,n,p}(t)$ is the acceleration
- $\Omega_{m,n,p}(t)$ the obstacle domains

By looking for the minimum $\delta(t)$ variation, it is possible to determine the complete trajectory profile of chords vibrations.

$$\Gamma(t) = f(\delta_{t_1}, \delta_{t_2}, \dots, \delta_{t_n})$$

where n is the number of isochronous surfaces with mini-nodes that have either chords vibrations or the probability of chords vibrations.

Since the trajectory to be traveled is not completely known, the chords vibrations have different propagation probabilities. For the path already traveled, the probability is 100%. For the path that is yet to be traveled, the chords vibrations propagation probability, will have the following form:

$$\Gamma_t = f(\rho_{t_1}, \rho_{t_2}, \dots, \rho_{t_n})$$

where:

- Γ_t is the trajectory
- ρ_t is the chords vibrations propagation probability
- t is the time step

If the ρ_t is higher then a certain threshold $\rho_{t_{min}}$, then the corresponding isochronous surface is selected as a segmentation surface.

As a consequence the isochronous trajectory is expanded to include the chords vibrations and the chords vibrations propagation probability:

$$\Gamma_t = f \left((x_t, y_t, z_t), \left(\begin{matrix} K_{11} & K_{12} & \dots & K_{1n} \\ & K_{22} & \dots & K_{2n} \\ & & \dots & \\ & & & K_{nn} \end{matrix} \right), \hat{f}(x, y, z), P(x_1 < S_n < x_2), \delta_{t_n}, \rho_{t_n} \right) \quad (6)$$

4. Measurements

Instrumentation used in this study for the trajectory measurements consisted of a compass HDMM01 and a ArduinoUno. The instruments used the factory calibration with no modifications. The sensor and ArduinoUno were fixed in a case that was placed on the vehicle floor. The 20 ms sample time between isochronous nodes was chosen in order to allow multiple readings within the target speed range of 0 to 50km/h. Also, the same driver was used to gather the data and the same trajectory was chosen to illustrate the method. Different hours and days were used to have a good sample of traffic influence on the trajectory isochronous patterns.

The measurement system is implemented with the sensor connected with a two wire (i2C) cable to the Arduino. The data from compass is the raw result of measured acceleration along a reference axis. No correction is done on the signal, no zero bias, zero scale factor or random error correction is applied.

Compass module	
Type	HDMM01, Dual-axis Magnetic Sensor Module
Effective measurement range	± 5 gauss
Sensitivity	512counts/gauss @3.0V at 25°C
	MIN: 461 counts/gauss
	MAX: 563 counts/gauss
Supply Voltage	2.7 ... 5.25 V
Noise Density	1 ~ 25Hz, RMS, 600 μ gauss
Accuracy	± 5 deg
Mechanical properties of the module	
L \times l \times H	16,20 \times 12,30 \times 2,25 (mm)

From these readings it was possible to derive the specific trajectory horizon of predictive isochronous paths. The trajectory graph consists of nodes, which are usually represented as circles, and edges, which are represented as line segments connecting the nodes.

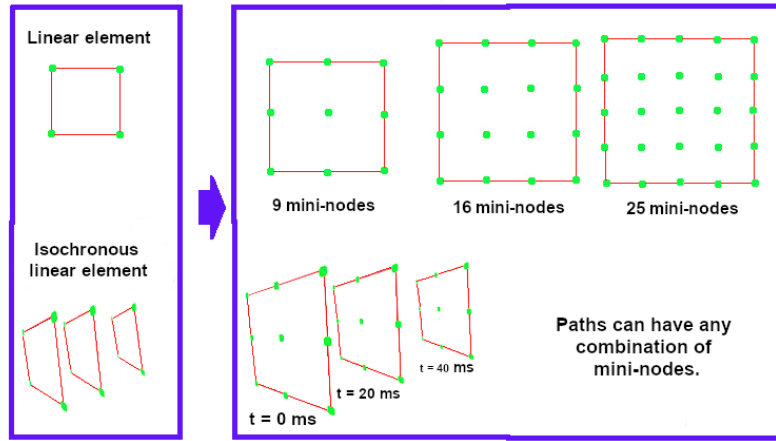


Figure 6: Each isochronous surface can have multiple mini-nodes

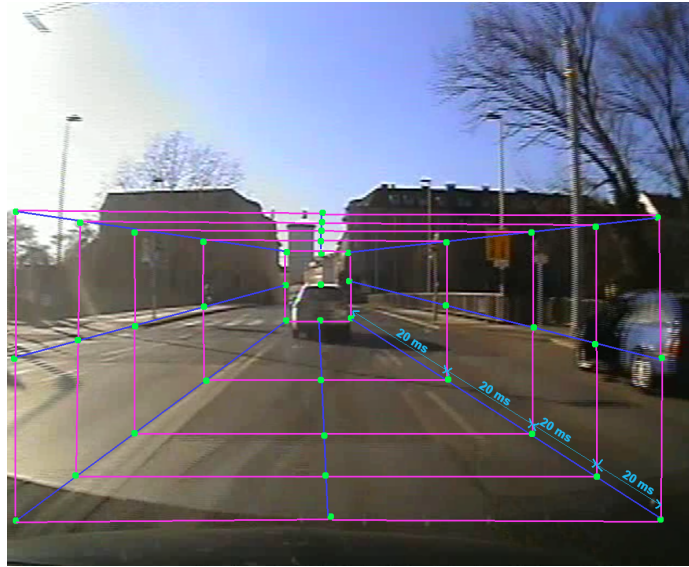


Figure 7: Segment of vehicle path with isochronous surfaces

The forward direction can be derived from the corners of the isochronous surface or it can be derived from the center of the isochronous 9 mini-nodes representation. With the 16 mini-nodes representation, it is possible to have an increased precision for the trajectory prediction. Adding mini-nodes to each isochronous surface leads to improved prediction accuracy in situations like intersections or vehicle lane changing.

From the increased number of mini-nodes for each isochronous surface it is possible to reverse to less complex isochronous surface representation when the vehicle is approaching a stop light or an immediate standstill situation.

Each node of the trajectory map represents a decision point, such as, “Must I make a left or a right turn?”. The corners of isochronous surface will indicate if the probability of a left or right turn decision is going to be increased or not. The predictive paths can be evaluated according to the benefits they offer, like reaching the destination with current vehicle energy reserves or improve operating parameters if the path adds a delay of minutes. From these paths, the optimal plan can be one that maximizes the vehicle state of operation.

Each mini-node and isochronous surface can give a certain probability that the vehicle will follow a specific path. A straight line trajectory can be represented with the green color, while an approaching vehicle path change can be represented from yellow to red. Previous compass data is used to provide predictive trajectory isochronous surfaces. Based on the compass data, the complexity of the isochronous surfaces can be reduced if there is a high probability that the vehicle will follow previous recorded paths.

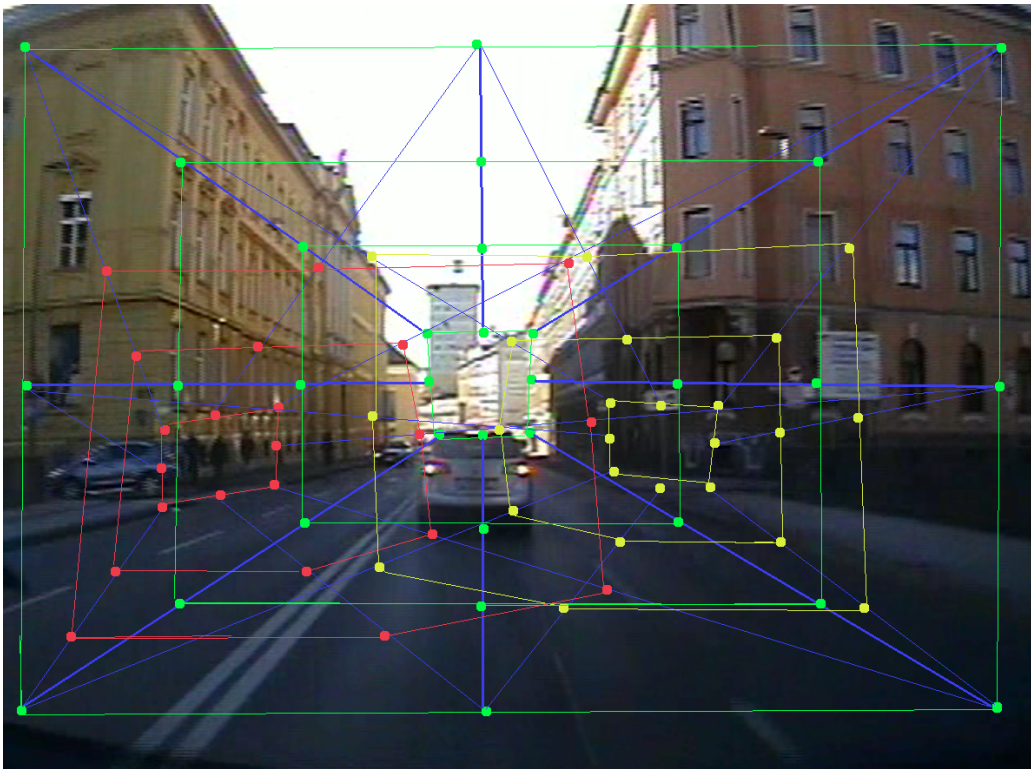


Figure 8: Multiple isochronous trajectories.
Green (most likely), yellow (back-up path), red (not allowed)

In figure 8, the vehicle will most likely follow the path no.1, as indicated by the color green in the isochronous trajectory surfaces. Nevertheless the path estimation can consider also path no.2 (red) and path no.3(yellow) as possible vehicle trajectories. The path no.2 (red) is a forbidden trajectory path. By having the video data and the compass data it is possible to validate the predictive trajectory isochronous surfaces.

If the uncertainty level for a specific trajectory path reaches a certain level, it is possible to increase the number of mini-nodes for each isochronous surface. Thus, every small change in the sensor value can be captured and the prediction horizon for the vehicle trajectory can be increased.

The compass data can be used to determine also other variables that can characterize the vehicle behavior on the selected path:

- speed and shifting: slipping in and out of gears
- acceleration and deceleration: the way a vehicle is maneuvered can influence how other vehicles react
- changing lanes: it is possible to recognize lateral movements created by a vehicle and differentiate a left-lane change from a right-lane change

The equation 6 provides the necessary information to calculate and predict the trajectory path Γ_t . For day 1, since the profile of trajectory path is not yet known, the information

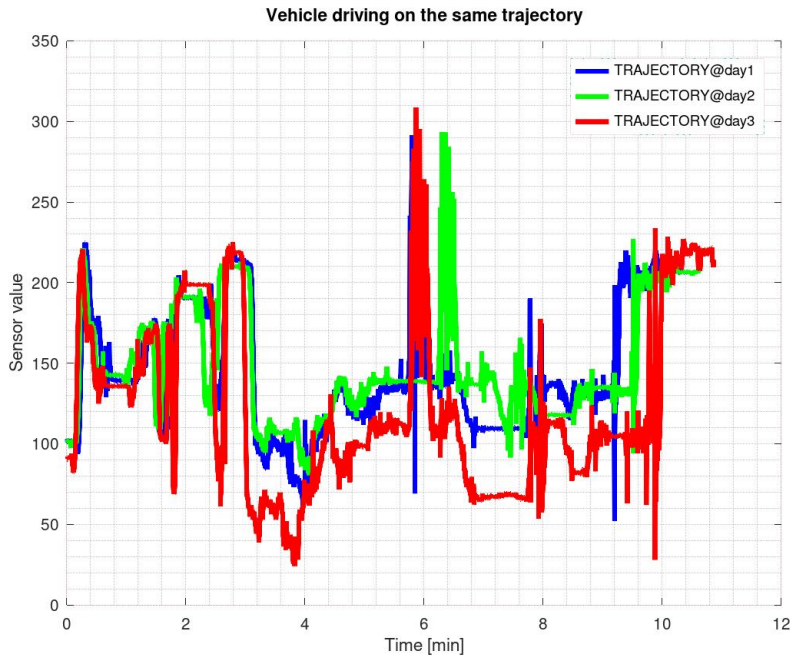


Figure 9: Measurement results

about possible obstacle domain Ω can only be received from the road infrastructure. In case of such obstacle domains Ω in day 1, the Γ_t will be prepared to encounter them in day 2 and day 3. In a similar way, the random segmentation surfaces, the correlation distribution matrix for them, the probability of random segmentation surfaces, the chords vibrations and the chords vibrations propagation probability are predicted with some degree of freedom in day 1. For day 2 and day 3 the accuracy of the Γ_t predictability increases.

5. Conclusions

In the present paper it was demonstrated the usage of predictive isochronous trajectories based on recorded compass sensor data. The measurement system is simple to construct, portable, cost efficient, low power consuming and reliable.

By using predictive isochronous trajectories it is possible to determine vehicle path within a predefined time horizon. The mini-nodes that constitute the isochronous surfaces can provide great accuracy in predicting the desired trajectory.

At the same time, energy savings can be obtain if the vehicle has a trajectory horizon estimation algorithm. Multiple energy systems can be synchronized to work together to achieve the best energy efficiency for the planned trajectory.

6. References

References

- Marshall Bern and Paul Plassmann. Mesh generation. In *HANDBOOK OF COMPUTATIONAL GEOMETRY. ELSEVIER SCIENCE*, pages 291–332, 2000.
- V. Boskoff. *Probleme practice de geometrie*. Editura Tehnică, București, 1990.
- Joseph Joshua and et al. A bayesian nonparametric approach to modeling motion patterns. *Autonomous Robots*, 2011.
- Manavender R. Malgireddy, Ifeoma Nwogu, and Venu Govindaraju. Language-motivated approaches to action recognition. *Journal of Machine Learning Research*, 14(30):2189–2212, 2013. URL <http://jmlr.org/papers/v14/malgireddy13a.html>.
- D. Mayne, J. Rawlings, C. Rao, and P. Sokaert. Constrained model predictive control: Stability and optimality. *Automatica*, 2000.
- Franziska Meier, Evangelos Theodorou, and Stefan Schaal. Movement segmentation and recognition for imitation learning. In Neil D. Lawrence and Mark Girolami, editors, *Proceedings of Machine Learning Research*, volume 22, pages 761–769, La Palma, Canary Islands, 21–23 Apr 2012. PMLR. URL <http://proceedings.mlr.press/v22/meier12.html>.
- C. Moineagu. *Statistica*. Editura Didactică și Pedagogică, București, 1976.
- Dale Peterson, Jason Moore, Danique Fintelman, and Mont Hubbard. Low-power, modular, wireless dynamic measurement of bicycle motion. *Procedia Engineering*, 2:2949–2954, 06 2010. doi: 10.1016/j.proeng.2010.04.093.
- POLLIN. Kompassmodul hdmm01. Available at <http://www.pollin.de/>, June 2020.
- SAE. Vehicle dynamics terminology j670-200801. Available at <https://www.sae.org/standards/content/>, June 2020.
- M. Sandu. *Mecanică teoretică*. Editura Didactică și Pedagogică, București, 2002.
- Zhanpeng Shao and Youfu Li. Integral invariants for space motion trajectory matching and recognition. *Pattern Recogn.*, 48(8):2418–2432, August 2015. ISSN 0031-3203. doi: 10.1016/j.patcog.2015.02.029.
- Alla Sheffer, Emil Praun, and Kenneth Rose. Mesh parameterization methods and their applications. *Foundations and Trends® in Computer Graphics and Vision*, 2(2):105–171, 2007. ISSN 1572-2740. doi: 10.1561/06000000011. URL <http://dx.doi.org/10.1561/06000000011>.